# Sperm motion in a microfluidic fertilization device

**M. d. C. Lopez-Garcia · R. L. Monson · K. Haubert ·
M. B. Wheeler · D. J. Beebe**

**Abstract** Microfluidics has shown promise as a new
platform for assisted reproduction. To assess the potential
of microfluidics for fertilization, we studied sperm and fluid
motion in microchannels to better understand the flow
characteristics in a microfluidic device, how sperm inter-
acted with this flow, and how sperm–oocyte attachment
occurs in the device. There is a threshold fluid velocity
where sperm transition from traveling with the fluid to a
regime in which the sperm can move independently of the
flow. A significant population of sperm remained in the
inlet well area. Based on the lack of progressive forward
movement, it was presumed that these sperm may have
defects. Also of extreme interest was the tendency of sperm
to travel along surface contours. These observations
provide an improved understanding of sperm motion in
microchannels and provide a basis for improved device
designs that take advantage of the sperm/flow and sperm/
geometry interactions.

**Keywords** Sperm · *In vitro* fertilization · Microfluidic ·
Sperm motility · Microchannel

M. d. C. Lopez-Garcia
University of Wisconsin—Madison,
2139 Engineering Centers Building, 1550 Engineering Dr.,
Madison, WI 53706, USA
e-mail: mlopezgarcia@wisc.edu

R. L. Monson
University of Wisconsin—Madison,
444 Animal Science Building, 1675 Observatory Dr,
Madison, WI 53706, USA
e-mail: monson@calshp.cals.wisc.edu

K. Haubert
University of Wisconsin—Madison,
2141 Engineering Centers Building, 1550 Engineering Dr,
Madison, WI 53706, USA
e-mail: khaubert@facstaff.wisc.edu

M. B. Wheeler
University of Illinois, Urbana-Champaign,
1207 West Gregory Dr.,
Urbana, IL 61801, USA
e-mail: mbwheeler@uiuc.edu

D. J. Beebe (✉)
University of Wisconsin—Madison,
2142 Engineering Centers Building, 1550 Engineering Dr,
Madison, WI 53706, USA
e-mail: djbeebe@wisc.edu

## 1 Introduction

Scientists have been studying *in vitro* fertilization (IVF) for
more than half a century. The first successful IVF offspring
was in rabbits in 1959. This experiment involved the
placement of rabbit ova into small 1.5 mL capacity Carrel
flasks that contained uterine sperm (Chang 1959). Today,
though fertilization is not carried out in flasks, the tools used
for IVF are largely unchanged (Clark et al. 2005). IVF is
most often done using a microdrop technique, wherein
technicians pipette cells into drops (50–100 μL) covered in
light mineral oil in a Petri dish and transfer the cells by hand
for all the steps in IVF (Fischer-Brown and Monson 2006).
This manual method may create unnecessary trauma to the
cells. In addition, there are species-specific problems that
occur only in the microdrop *in vitro* technique. An example is
the occurrence of polyspermy in porcine IVF when utilizing
the microdrop technique (Abeydeera 2002; Clark et al. 2005).

In the last 10 years microfluidics has been explored as a
tool for IVF. One motivation for the use of microchannels is
that they provide a geometrically constrained microenviron-

ment that may be more similar to the in vivo microenvironment (Beebe et al. 2002a, b). In addition the flow properties in microfluidics may enable a more predictable delivery of sperm to oocytes during IVF (Suh et al. 2006). Lih et al. presented a device in 1996 where microchannels were extended from the traditional microdrop (Lih et al. 1996). In this case, oocytes were placed in sidewells and sperm was added to the center drop with the purpose of concentrating the motile sperm at the site of fertilization. Also in 1996, Kricka and Wilding presented a device for fertilization in which sperm swam through a tortuous channel toward an oocyte at the other end. The fastest and strongest sperm would be naturally selected according to their ability to negotiate the channel and those sperm would fertilize the egg (Kricka and Wilding 1996). Since then, various research groups have seen the potential for microfluidics in IVF for important tasks such as sperm sorting and qualitative selection (Lih et al. 1996; Cho et al. 2003; Schuster et al. 2003; Suh et al. 2005; Seo et al. 2007), zona pellucida removal (Zeringue et al. 2005), oocyte cumulus removal (Zeringue and Rutledge 2004), and fertilization (Clark et al. 2005; Suh et al. 2006). The prospect of an integrated device that includes all of these steps and accomplishes a large part, if not all, of the IVF procedure with minimal operator intervention would mean less variance in the protocols, increased efficiency, and less handling stress on living cells (Suh et al. 2005; Thompson 2006).

Attempts to carry out IVF in microfluidic devices have yielded encouraging results (Kricka and Wilding 1996; Clark et al. 2005; Suh et al. 2006). Suh et al. achieved similar penetration rates in their devices compared to the center-well technique, but with a lower concentration of sperm. Clark et al. achieved a significant increase in monospermic penetration for porcine IVF in their micro-channels in comparison to the microdrop. However, the mechanisms that provide improvements are not clear.

The IVF devices described by Clark et al. (2005), possess numerous attributes that make them amenable to direct observation of these mechanisms. Relevant features include: (1) a clear glass bottom which allows for visualization of the cells; (2) facility to track the movements of the cells, as they swim down a channel; (3) convenience for use with fluorescent, bright-field and phase contrast microscopy, or methods such as cell vitality staining; (4) self contained design permits use in conjunction with an incubated microscope stage for long term studies. Use of an incubated microscope stage is essential to insure that observations accurately reflect what takes place under normal circumstances, and that cells are not being affected by sub-optimal temperature and atmosphere.

In this study our goal was to observe sperm motion in microchannels in an attempt to better understand how they behave and interact with the device. In particular, we studied the flow velocity and profile, how this flow affects sperm behavior, if there is a location within the device where sperm accumulate, and when or how sperm attachment to the oocyte occurs. This information will enable scientists and engineers to better understand the central mechanisms and improve device design. To obtain this information, the following steps were taken: (1) baseline flow of the fluid in the channel was studied using particle tracking and particle image velocimetry (PIV) techniques; (2) baseline flow information was combined with sperm flow information to understand sperm-device interactions; (3) sperm attachment to the oocyte was determined with respect to the baseline flow. During each of the previous steps, the effect of the device geometry on sperm behavior was observed. These steps are illustrated in Fig. 1. Bovine sperm was used for all of these experiments.

## 2 Materials and methods

A compilation of the experiments carried out can be seen in Table 1.

### 2.1 Fabrication of IVF devices

The methods for making the IVF microfluidic device was previously reported (Clark et al. 2005). Briefly, channel structures were fabricated from polydimethylsiloxane (PDMS) using standard photolithography and micromold-
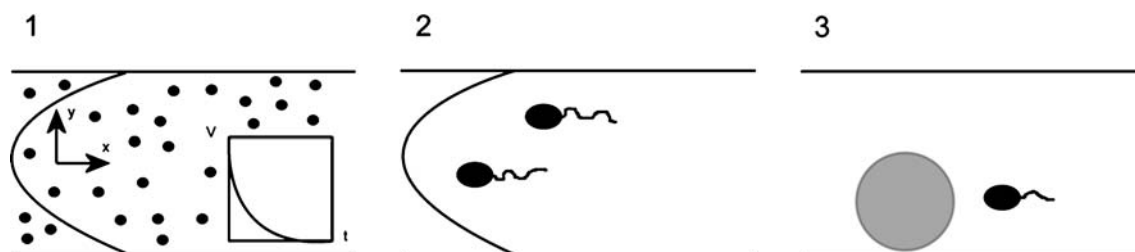


**Fig. 1** Experimental steps to better understand sperm behavior in microchannels. *Horizontal parabola* represents expected flow profile. *1* Representation of measurement of baseline flow with respect to time and distance from the wall, by studying particle displacements. *2* Observations of interactions between sperm and flow, and *3* Interaction conditions of oocyte and sperm with respect to the flow. Drawings are not to scale

**Table 1** Description of experimental setups

| Purpose | Setup |
|---|---|
| Baseline flow characteristics | Channel with media and fluorescent beads |
| Flow and sperm interaction | Channel with media and sperm. Variations include: |
| | Two device geometries |
| | Added fluorescent beads to compare flow and sperm paths |
| | Added glass beads to simulate the presence of oocytes |
| Sperm and oocyte interaction | Channel with media, sperm, and oocytes |

ing techniques. These were then plasma bonded to a glass microscope slide, which constituted the base of the device and the bottom surface of the microchannels. See Fig. 2 for a diagram of devices.

The device consists of a 250 μm tall by 1,000 μm wide microchannel with an inlet to insert fertilization media, oocytes, and sperm, and an outlet to let air out as these elements are inserted (Fig. 2(a)). Midway through the channel is a constriction area. The constriction area can be described as a wall that comes down from the top of the channel and leaves an opening of 20 μm above the bottom of the channel that serves as a "parking spot" for the oocytes (Fig. 2(b)). The 20 μm opening, that prevents the oocyte from moving to the outlet but allows for sperm flow, widens into an oval shape (Fig. 2(c)) that extends past the sides of the channel. his was one of the device geometries used for the experiments described in this paper. In addition, another type of device geometry was used which can be described as the straight configuration (see Fig. 2(d)). This device also has a wall that comes down from the top of the channel and extends down to 20 μm above the bottom of the channel, but this constriction does not extend outward from the main channel.

### 2.2 Fertilization medium preparation

The fertilization medium consisted of IVF-TALP (Bio-whittaker, Walkersburg, MD) supplemented with 0.22 mM sodium pyruvate, 25 μg/ml gentamicin sulfate and 6 mg/ml essentially fatty acid free bovine serum albumin (BSA). The albumin concentration of 6 mg/ml essentially fatty acid free bovine serum albumin (Sigma A-8806) in IVF TALP (Cat#BSS-010-D, Specialty Media, Phillipsburg, NJ) is the gold standard protocol adapted and used at the University of Wisconsin and has successfully produced hundreds of thousands of embryos and thousands of live healthy calves since its initial usage (Parrish et al. 1985).

For experiments with fluorescent beads, the fertilization medium was mixed with a 2% solid solution of 1 μm

diameter Molecular Probes Flourospheres of a Nile Red emission in order to obtain a 1% volume concentration of the bead solution.

### 2.3 Preparation of sperm

Semen from five different bulls was used during the experiments to ensure that the observed phenomenon is not the effect of a particular bull. Frozen-thawed sperm from commercially available bulls was used for the studies. Sperm were centrifuged at 700×g for 7 min in a discontinuous percoll gradient to separate the live from dead fraction (Parish et al. 1995). The supernatant of the
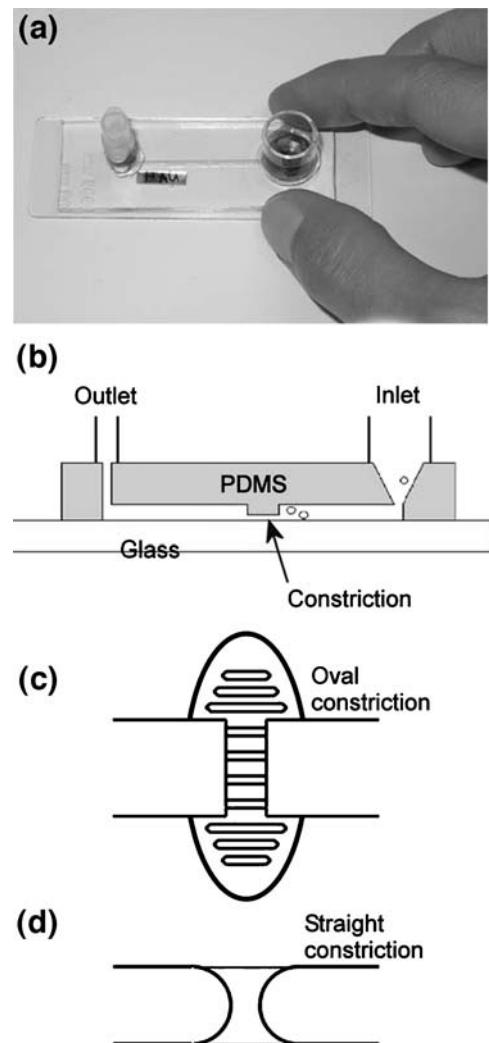


**Fig. 2** (a) Photograph of device. (b) *Side view* of microfluidic device used for fertilization. The device is fabricated with polydimethylsiloxane (PDMS) on a glass slide. The oocyte is parked by the constriction on the side of the inlet. Sperm is added through the inlet. (c) *Top view* of an oval constriction. Sperm can swim into the oval area that extends outside of the channel that is sustained by supports (*horizontal contours in oval*). This area is 20 μm high. (d) *Top view* of a straight channel constriction. Constriction is 20 μm in height. Drawings are not to scale

percoll was removed and 1 ml of TALP HEPES medium was added back to the tube and re-spun for a period of 2 min to facilitate removal of globulins or other materials remaining from the semen extender. A 1:20 diluted sample of sperm was placed onto a hemacytometer and the sperm concentration established. Once this concentration was known, a sperm suspension was prepared 2× of the desired final concentration so that 200 μL of the 2× suspension could be delivered to the inlet well resulting in a 1:1 dilution of 2× sperm suspension with the 200 μl of medium already contained within the channel. This dilution resulted in the final desired sperm concentration. It should be noted that in the microchannel, fluid flow properties and the nature of the fluids to slowly diffuse at the micro level, prevents dilution as would occur in a microdrop. Therefore, the desired concentration may not be uniform throughout the channel.

### 2.4 Preparation of oocytes

Mature bovine oocytes were purchased from Bomed, Inc. (Madison, Wisconsin). Ovaries were obtained from one or more abattoirs in Wisconsin, primarily from Holstein cattle. Oocytes were taken from antral follicles (>2 to 6 mm) and selected if a compact cumulus of several cell layers was present. Oocytes were processed in TALP-HEPES with 0.22 mM sodium pyruvate, 25 μg/ml gentamicin sulfate and 3 mg/ml BSA. Oocytes (50/vial) were incubated for 20 to 24 h in 2 ml vials filled with maturation medium that was equilibrated in 5% carbon dioxide in air (39°C, humidity level above 90%). Maturation medium consisted of TC199 with Earle's salts supplemented with bovine LH and FSH from Sioux Biochemical (Sioux Center, IA, 51250), 0.22 mM sodium pyruvate, 25 μg/ml gentamicin sulfate and 10% heat inactivated fetal calf serum. Oocytes were incubated in maturation medium for a period of 20–24 h. Mature oocytes were washed three times in TALP-HEPES with 0.22 mM sodium pyruvate, 25 μg/ml gentamicin sulfate and 3 mg/ml BSA.

### 2.5 Imaging techniques

All of the imaging was done with an IX70 Olympus inverted microscope. UV lighting (555 nm) was used to image the fluorescent beads. The microscope was set up with a stage capable of being manually leveled. A small incubation box with a glass bottom was developed that could be placed upon the microscope stage. This box maintained temperature, humidity, and $CO_2$ levels comparable to those in a standard incubator, permitting sperm and oocytes to be observed over the course of hours, with no detrimental effect. IVF devices were placed inside this box during the imaging procedures for all observations including the base flow analysis.

Still photography was carried out with a Diagnostic Instruments, Inc., SPOT 2.1.1; movies were taken with a PixeLINK PL-A741 Machine Vision Camera. For flow profiles, ten time-lapse images were taken at a frame rate of one fps at times $t=0$, 5, 10, 30, 60, and 90 min. For sperm movies, a frame rate of 10 to 13.5 fps was used. Positioning of the SPOT 2.1.1 was controlled by Metamorph software. Movie imaging was controlled with PixeLINK OEM software.

Image analyses for flow profiles were carried out with two different software packages. Imaris Bitmap software was used to obtain flow velocities using particle tracking whereas DaVis LaVision PIV software was used to obtain flow profiles with the PIV time-series operation in a multi-pass setting from $256 \times 256$ for the first pass to $128 \times 128$ for the second pass.

### 2.6 General protocol

The empty device and the fertilization media were placed in a plastic box with a water reservoir and this box in turn was placed into an incubator. The incubator environment was set to an optimum fertilization environment at 38.5°C, 5% $CO_2$ and a humidity level above 90%. The purpose of this was to saturate the device walls with $H_2O$ and $CO_2$ and to thermally equilibrate the media and device with a cell friendly environment. Equilibration of both the empty device and medium also reduces the likelihood of bubble formation when the device is filled with medium. This is important because bubbles will hinder fluid flow within the channel. The devices, devoid of medium, were equilibrated to incubation conditions for a period of at least 2 h after which 200 μL of sterile pre-equilibrated fertilization medium was added via micro-pipette at the inlet of the device. A sterile 1 cc tuberculin syringe was attached to the outlet luer of the device and gentle suction was applied to draw the medium into the inlet through the channel, across the constriction region and into the outlet. After adding the medium, devices were placed back into the incubator for 1 h to allow medium to reach an equilibrium static level across the entire device. Prior to proceeding, the devices were removed briefly from the incubator to inspect for the presence of bubbles at, or near the constriction region, via microscopy. In the event that bubbles had formed, additional suction was applied to attempt to move or remove them. When oocytes or 90 μm glass beads were being used, they were loaded into the channel at this point. Devices were then transferred to the incubation box on the microscope stage and allowed to reestablish a static state before sperm and/or additional medium were added for observation.

The devices, devoid of medium, were equilibrated to incubation conditions for a period of at least 2 h after which

200 μL of sterile pre-equilibrated fertilization medium was added via micro-pipette at the inlet of the device. A sterile 1 cc tuberculin syringe was attached to the outlet luer of the device and gentle suction was applied to draw the medium into the inlet through the channel, across the constriction region and into the outlet. After adding the medium, several devices were placed back into the incubator for 1 h to allow medium to reach an equilibrium static level across the entire device. Prior to proceeding, the devices were removed briefly from the incubator to inspect for the presence of bubbles at, or near the constriction region, via microscopy.

### 2.7 Base flow studies

In the base flow studies, the device was originally filled with medium containing fluorescent beads. Once the device was in the incubated stage, an additional 200 μL of fluorescent beaded media was added at the inlet, as a substitute for the sperm volume, to create flow. The initial pictures were taken within seconds, and then the incubation box on the microscope stage sealed, for further imaging.

### 2.8 Sperm/flow interactions

The general protocol was followed with the optional step of inserting glass beads to simulate the presence of oocytes. Approximately ten 90 μm diameter glass beads were injected into the channel containing the initial medium. The device was then slightly tilted so that the glass beads would slide towards the constriction area. The device was placed into the incubation box on the microscope, and a 200 μL aliquot of the sperm sample (in place of the additional beaded medium) was added to the inlet. Imaging was then carried out. Some of the experiments were also carried out with fluorescent beads in the initial volume of media so as to visualize flow and sperm movement at the same time.

### 2.9 Sperm incubation with oocyte studies

The same protocol as described above was followed with the exception that oocytes where used in place of the 90 μm glass beads. The oocytes were inserted into the channels using a pulled glass capillary micropipette. They were allowed to settle on a level surface for approximately 2 min. The device was then placed on an approximate 5° angle to the horizontal for 5 min to allow the oocytes to travel to the constriction region under the force of gravity. The position of the oocytes at or near the constriction region was confirmed via microscopy prior to sperm addition. The rest of the preparation was carried out as described in the sperm/flow interaction studies.

## 3 Results

This study presents the behavior of sperm observed within a microfluidic *in vitro* fertilization (IVF) device, with the intent of assisting reproduction biologists and design engineers in understanding how microfluidic device features influence sperm behavior and fertilization.

In our experiments, the baseline flow profile of the fluid was studied within the channel and this information was used when evaluating sperm behavior within the channel. In addition, observations were made of the interaction of the sperm with the oocyte in relation to the flow profile. Also, the effect of device geometry on sperm behavior was examined.

### 3.1 Baseline flow profiles and velocities

The baseline flow was studied by recording movies of the flow in the channel. The flow was visualized using fluorescent beads that were mixed with the medium. The displacement and the time between frames lead to flow information such as direction and velocity magnitude. The actual directions and velocities for the bulk fluid flow were obtained using the tracking software *Imaris*. Information on the flow direction for the constriction area was obtained with the particle image velocimetry (PIV) software *DaVis*. Previous experiments have shown flow behavior in a microchannel of similar size and indicate velocities are laminar (Brody et al. 1996; Beebe et al. 2002a, b). In the present study, the results concurred with previous work reported in the literature, and a laminar flow profile was corroborated (data not shown). In addition, the study of the flow profile over time showed an exponential decrease in velocity (data not shown) with the flow velocity reaching zero approximately 30 min after fluid addition. The data that was obtained correlates closely with a mathematical model for flow decay for gravity driven flow in a channel with an open reservoir in each end[1].

The velocity profile in the constriction area has a more complex profile. As shown in Fig. 3(left) the flow comes straight from the channel and fans out into the constriction area. The raw image of the flow, Fig. 3(right), in this area portrays the same observation showing more clearly how the flow splits from the larger channel into the smaller constriction channels. The split can be seen in the area that is indicated with a square. This flow is actually coming down before fanning out into the constriction area. The vectors close to the edges appear shorter not because flow

---

[1] For a general description of fluid relationships in microfluidics, refer to Chapter 9 in "Micromachined Transducers Sourcebook" by Kovacs (1998).
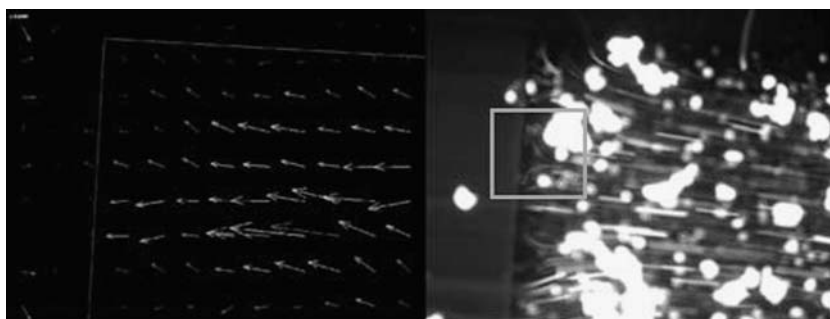
is slower there but because the images are 2D slices that do not include a vertical component.

### 3.2 Interaction of the sperm with the flow

After the characteristics of the flow were understood, experiments were conducted in the presence of live bovine sperm. Glass beads were used to simulate the presence of oocytes. Movies of the inside of the channel were recorded once the sperm were placed into the device.

Initially, the sperm swam in the same direction of the fluid flow. It is important to note that they were properly oriented and swimming, as opposed to simply being dragged by the flow (Fig. 4). This behavior was observed for the first 4 to 10 min of flow and corresponds to a flow velocity of 17 μm/s or higher. Once the flow velocity decreased below ~17 μm/s, the sperm were seen swimming in directions different than that of the flow. Figure 5 shows a stack of individual frames from one of the movies in which a sperm cell was captured turning to swim in the direction opposite to the flow.

### 3.3 Interaction of sperm with the oocytes

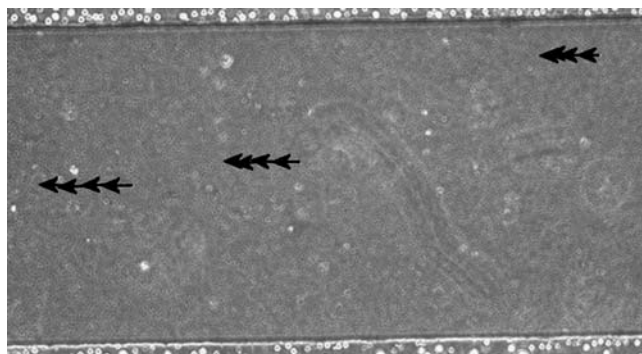In the final set of experiments actual matured oocytes were used in place of the large glass beads. The oocytes were placed into the device after the device had been filled with an initial volume of fertilization medium.

It was observed that during the initial portion of the flow, sperm tended to swim past the oocytes, often into the constriction area (see Fig. 6(a)). Once the flow rate decreased to that where the sperm begin to swim in directions different to the flow it was observed that the sperm cell began to attach to the oocyte almost immediately Fig. 6(b). Here we observed sperm approaching, although other sperm can be seen, that have already attached to the oocyte.

#### 3.3.1 Anecdotal observations

Although oocytes were at times very close to the sperm cells, sperm would often continue along their original path without initiating contact with the oocyte (observed at $t\sim$ 16 min and later).

Experiments were performed where the oocytes were substituted by glass beads. Even though the shape and texture of a real oocyte is much more complex than a simple glass bead, the experiment was done in order to get clues about whether there is chemotaxis between the sperm
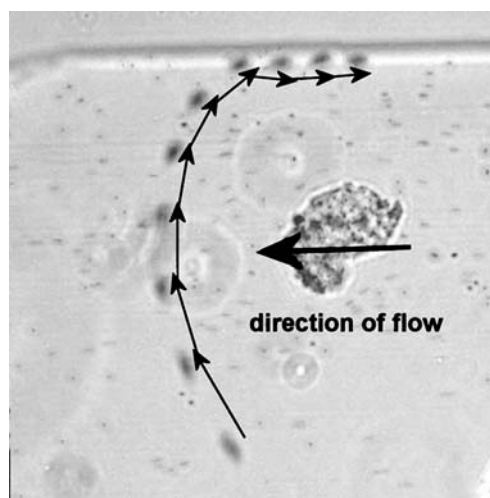


**Fig. 4** Sperm swimming with the flow. *Arrows* indicate location and trajectory of sperm. The sperm are seen swimming in a straight line as trapped by the velocity in that point of the profile. This image was taken 3 min after injection. *Each arrow* represents the movement of the sperm in 0.2 s



**Fig. 5** A sperm cell taking control of its own direction. The sperm at first comes from the direction of the flow (*right to left*) and then makes a U-turn to go in the opposite direction. This image was taken at $t=$ 10 min after injection. *Each arrow* represents the movement of the sperm in 0.2 s

Fig. 6 (a) Sperm missing the oocyte at $t=10$. (b) Sperm approaching the oocyte at $t=15$ min, after decrease of flow velocity. *Arrows* in both images represent the movement of the sperm in 0.1 s
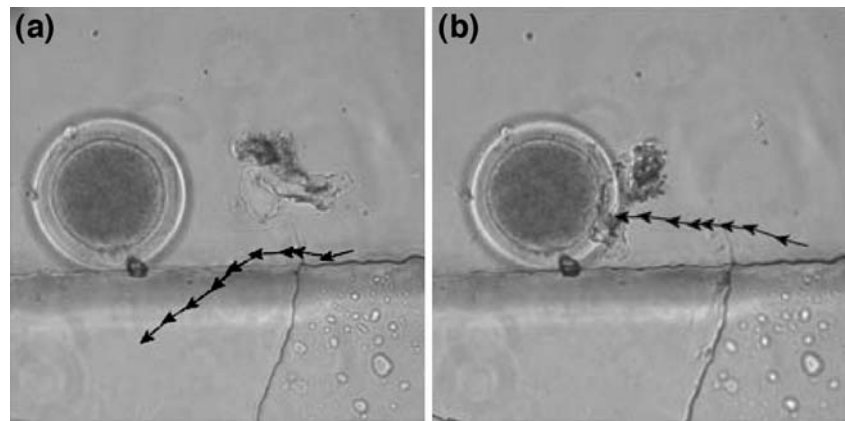


and the oocyte and also if there were any special effects from the disruption of the flow. In these experiments, it was observed that at times sperm cells would bump into the glass beads as if to test for the presence of an oocyte (observed at $t \sim 10$ min and later).

3.4 The effect of the device geometry on sperm behavior

One of the questions that were asked at the start of the study was: Do the sperm cells congregate in a particular location within the device? It was found that a substantial portion of the sperm remained in the inlet and did not depart into the channel area as shown in Fig. 7.

In addition, although there was not another location within the device where the sperm cells concentrated, it was seen that sperm tended to preferentially swim along the
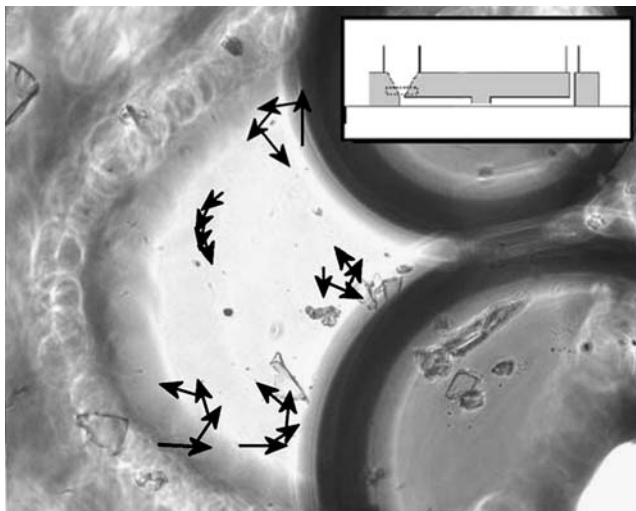


Fig. 7 Sperm swimming in the inlet area. These sperm tended to swim around in circles, indicating that they may have a motility defect. This image sequence was taken 17 s after injection. *Each arrow* represents the movement of the sperm in 0.2 s. Location of the sperm within the device is shown in *box on top left corner*. *Round shapes at right* of image are out of focus bubbles on the surface of the medium

walls (including floor and ceiling) and contours of the device. This occurred during flow and no flow. See Fig. 8.

4 Discussion

As was explained in the previous section, the baseline flow within the channel is laminar and had an exponential decay in velocity that approached zero at around 30 min, for the 200 µL additions used. When combining this knowledge with the observation of sperm movement within the channel, the sperm/flow interaction can be divided into two regimes. In the first regime, the sperm swim with the flow, or are impulsed. The word "impulsed" may be defined as a combination of "pushed" and "swimming ahead of the stream". In this regime the sperm may not be able to swim in other directions because the force of the flow may be too great for the sperm to cross streamlines in the laminar fluid flow. In the second regime, the sperm overcome the force of the flow and begin to swim in directions other (or independent from) than the flow. Some sperm may be able to take control sooner than the others. The transition from the first to second regime took place within the first ~10 min, which corresponds to a point in the flow profile with respect to time where there is slow flow that has not quite reached zero. Also, this second regime is where we observed that the sperm can begin to interact with the oocyte. We noticed that as soon as the sperm are in control of their direction, they are more likely to find and attach to the oocyte, than to swim past it. In other words, the sperm that finally attached to the oocyte were those that weren't trapped in the initial flow, they were the free-swimming sperm at later times. *In vivo* a similar situation occurs. The female tract experiences contractions that increases the flow of sperm and transports them to the site of fertilization. The first sperm to reach the site are not necessarily the ones that will fertilize the oocyte, because these cells might not have had time to capacitate and be physiologically prepared to do so. It has been suggested

**Fig. 8** Sperm swimming along walls and contours. The location of sperm within the device is indicated on the right. (**a**) Sperm swimming into the constriction area in the oval configuration. Image sequence taken at $t=$ 6 min. *Each arrow* represents the movement of the sperm in 0.2 s. (**b**) Sperm swimming into the constriction area of a straight channel. Image sequence taken at $t=12$ min. *Each arrow* represents the movement of the sperm in 0.2 s. (**c**) Sperm swimming against the contours of the oval configuration constrictions. Image sequence taken at $t=10$ min. *Each arrow* represents the movement of the sperm in 0.2 s. In (**c**) we can see sperm gliding from surface to surface
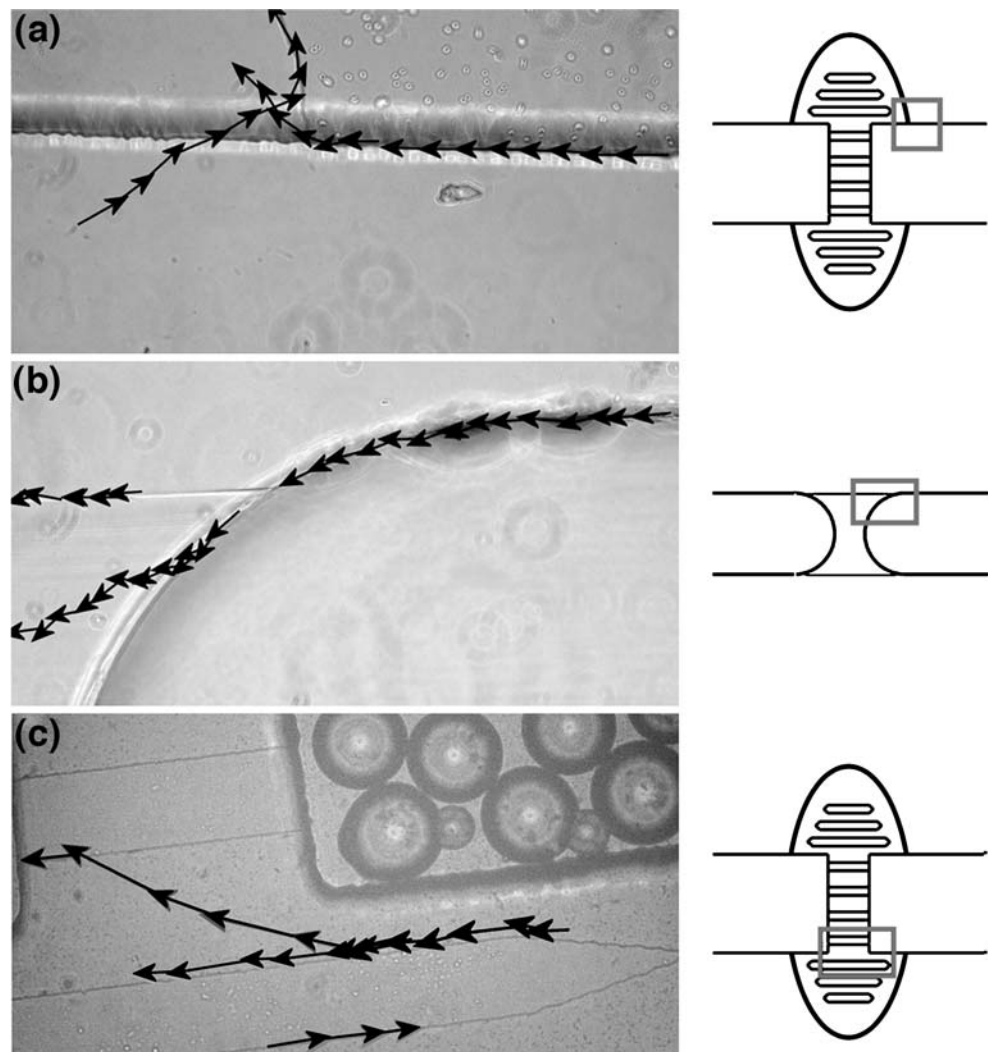


that the oocyte may be fertilized by sperm that have been stored away from the fast flow in crypts within the female tract and are released after the contractions cease (Suarez 2002; Rijsselaere et al. 2004; England et al. 2006). Our findings show that this event can be recreated in the microfluidic device and if necessary incorporated into the design by fabricating longer channels or by controlling the fluid flow velocity so that the sperm remain in their streamlines for the desired length of time.

As stated above, it is more likely that a sperm cell will interact with an oocyte when the flow diminishes. Once one sperm overcomes the force of the flow and attaches to the oocyte, other potent sperm become capable of overcoming the flow and were seen approaching the oocyte. Not all nearby sperm, however, find and attach or seem to be attracted to the oocyte. Some sperm continue on their trajectory and ignore the nearby oocyte. The behavior of the sperm was compared when in the vicinity of either glass beads or oocytes. For the glass bead case, the sperm cell would sometimes bump into the glass bead as if approach-

ing an oocyte. Both observations were made after the commencement of the second regime, where the sperm cells had control of their direction. No obvious difference was seen between the two cases. This observation gives no indication that there is an attraction mechanism of the sperm to an oocyte, although there have been many studies indicating that such chemotaxis exists. Eisenbach and Ralt (1992) and Eisenbach (1999), both provide reviews on this topic. The microfluidic device may provide a good system to study this age old question but a more quantitative study would be needed.

The geometry of the device also played an important part in the sperm behavior within the channel. For example, it was observed that in the inlet area of the device, there was a high sperm concentration. We did not observe sperm sticking to the walls of the device therefore, this possibility was discarded. The sperm that were viewed in this area had the characteristic of swimming in circles, which is an indication of poorly functioning sperm. This observation leads us to think that the inlet area may serve as a cut-off

for defected sperm. A possible explanation is that dead or defective sperm that were not washed out of the inlet by the flow remain in the inlet because of their circular swimming motion reduces the chances that they will encounter the channel. Note that the channel opening represents 10% of the well circumference. A similar conclusion was reached by Lih et al. (1996), with their motile sperm device. In their studies, they were able to concentrate motile sperm in the side channels because the non-motile sperm remained in the central droplet, where the sperm sample was injected. This can be related to what happens *in vivo* in that the female tract contains crypts that as well as acting as sperm cell reservoirs, as mentioned above, also serve the functionality of an initial selection mechanism for the sperm that will reach the site (Rijsselaere et al. 2004).

The sperm purification capacity of the device can also be compared to the integrated microfluidic system for separation of motile sperm by Cho et al. In this work, they began with a sperm sample that contained motile and non-motile sperm and collected motile sperm at the end of the channel. The motile sperm swam out of their initial stream to a secondary flow of media while debris and non motile sperm were trapped in the initial stream, thus occurs separation of motile and non motile sperm (Cho et al. 2003; Schuster et al. 2003). It should be noted that the velocities in the study carried out by Cho and Schuster are much less than the ones presented here. The purification mechanism between the two devices differs in that in Cho's device the nonmotile sperm are trapped in a stream while in the device presented here, the nonmotile sperm are trapped in a chamber-like area (the inlet).

Having a constriction area that holds the oocyte in a given position but provides additional channel space behind the oocyte also provided extra space for the sperm to swim and not over-concentrate in the near vicinity of the oocyte. This could have applications in reducing polyspermy in those species where that is a common problem. It is important to do experiments with these species and to investigate the influence of sperm motility.

Another case in which the geometry seems to play a key role in sperm behavior comes from the observation that sperm showed a preference for swimming near walls and contours. This also occurred after the sperm were able to take control of their direction. In our devices, the walls and contours act as guides for the direction in which the sperm will swim. This may also be what happens in vivo but has not been observed since the technology to do so is not available. One explanation is that the oocytes are not free floating in the middle of the fluid, but are sitting next to a wall. The sperm in vivo may also follow a surface to find them. The circumstance of sperm swimming by surfaces was first documented by J. Dewitz in 1886 (Dewitz 1886), later quantified by Lord Rothschild in 1963 (Rothschild

1963), and again by Winet et al. in 1984 (Winet et al. 1984). There are multiple theories of why this tendency occurs, among them a hydrodynamic interaction between the sperm cell and the surface (Rothschild 1963), a hydrofoil effect caused by the head shape and flagellar wave (Woolley 2003) (for the case of planar waves), and a three-dimensional component of the flagellar wave that tends to keep spermatozoa close to interfaces (Cosson et al. 2003). The purpose of this behavior *in vivo* (and whether it exists or not) may still be unknown, however, *in vitro*, this is a phenomenon that can be exploited. The tendency for the sperm to swim against surfaces is a feature that is not taken advantage of in the microdrop method. Knowledge of this behavior could be useful because with today's technology we can control geometry on the microscale and may be able to direct sperm to oocytes by designing devices with ledges, ridges, and guides that lead sperm to desired locations. This finding has applications not only in fertilization, but in sorting and in other *in vitro* production (IVP) steps for IVF sperm preparation, and can be applied in the design of integrated, automated devices. None of the current microfluidic devices that have been designed for in-vitro production take advantage of the sperm guiding capability by engineered contours.

Before concluding, it may be noted that sperm behavior in response to capacitation events and hyperactivation could impact sperm direction and movement. However, standard incubation conditions of 38.5°C temperature, >95% relative humidity and 5% carbon dioxide in the previously described fertilization medium has resulted in numerous publications describing complete bovine sperm capacitation, acceptable embryonic development rates, pregnancy rates and live healthy offspring. Although we did not specifically attempt to identify the hyperactivation potential of sperm, no characteristic figure-8 patterns of movement or irregular flagellar movement common with super-hyperactivated sperm were notable, not even in the inlet.

The devices tested here have already been proven successful for IVF (Clark et al. 2005). Now, the observations presented here can be used to design improved devices for IVF. For example, we could create sperm guides with walls and minimize the flow near oocytes to allow sperm to attach. We could control when the sperm attach by regulating the local flow rate and use the channel geometry studied here (channel before and after the oocyte) to keep a low sperm concentration around the oocyte for cases where the species is prone to polyspermy. We can also manipulate the quality of the sperm that can contact the oocyte by taking advantage of the "cut-off" effect of the inlet region has on defective sperm.

In conclusion, the phenomenon presented here although mostly qualitative, show that microfluidic devices can be a

powerful tool in IVF. The observations presented are important for the design of the improved devices with which we can provide guidance, purification, and temporal control during IVP. Future work should include more quantitative data that characterizes these interesting observations.

# References

L.R. Abeydeera, Theriogenology **57**, 257 (2002)

D.J. Beebe, G.A. Mensing et al., Annu. Rev. Biomed. Eng. **4**, 261 (2002a)

D.J. Beebe, M.B. Wheeler et al., Theriogenology **57**, 125 (2002b)

J.P. Brody, P. Yager et al., Biophys. J. **71**, 3430 (1996)

M.C. Chang, Nature **184**(4684), 466 (1959)

B.S. Cho, T.G. Schuster et al., Anal. Chem. **75**(7), 1671 (2003)

S.G. Clark, K. Haubert et al., Lab Chip **5**, 1229 (2005)

J. Cosson, P. Huitorel et al., Cell Motil. Cytoskelet. **54**, 56 (2003)

J. Dewitz, Archiv fur der Gesellschaft Physiologisch **38**, 358 (1886)

M. Eisenbach, Rev. Reprod. **4**, 56 (1999)

M. Eisenbach, D. Ralt, Am. J. Physiol. **262**, C1095 (1992)

G.C.W. England, C.M. Burgess et al., Theriogenology **66**(6–7), 1410 (2006)

A. Fischer-Brown, R.L. Monson, Laboratory protocol for the production of in vitro matured, fertilized, and cultured bovine embryos (University of Wisconsin—Madison, Madison, 2006)

G.T.A. Kovacs, *Micromachined Transducers Sourcebook* (McGraw-Hill, New York, 1998), pp 779–796

L.J. Kricka, P. Wilding, Pure Appl. Chem. **68**(10), 1831 (1996)

C.H. Lih, M. Obasaju et al., J. Assist. Reprod. Genet. **13**(8), 657 (1996)

J.J. Parish, A. Krogenaes et al., Theriogenology **44**, 859 (1995)

J.J. Parrish, J.L. Suskoparrish et al., Theriogenology **24**(5), 537 (1985)

T. Rijsselaere, A. Van Soom et al., Reproduction **128**(6), 801 (2004)

L. Rothschild, Nature **198**(4886), 1221 (1963)

T.G. Schuster, B.S. Cho et al., Reprod. Biomed. Online **7**(1), 75 (2003)

D.-b. Seo, Y. Agca et al., Microfluid Nanofluid. (2007)

S.S. Suarez, Reprod. Domest. Anim. **37**(3), 140 (2002)

R.S. Suh, S. Takayama et al., J. Androl. **26**(6), 664 (2005)

R.S. Suh, X. Zhu et al., Hum. Reprod. **21**(2), 477 (2006)

J.G. Thompson, Theriogenology **67**, 16 (2006)

H. Winet, G.S. Bernstein et al., J. Reprod. Fertil. **70**(2), 511 (1984)

D. Woolley, Reproduction **126**, 259 (2003)

H. Zeringue, J.J. Rutledge, Lab Chip **5**, 86 (2004)

H.C. Zeringue, M.B. Wheeler et al., Lab Chip **5**, 108 (2005)